Complexome analysis of the nitrite-dependent methanotroph *Methylomirabilis lanthanidiphila*

Wouter Versantvoort[1*], Sergio Guerrero-Castillo[2], Hans J.C.T. Wessels[4], Laura van Niftrik[1], Mike S.M. Jetten[1], Ulrich Brandt [2,3], Joachim Reimann[1] and Boran Kartal[5*]

[1] Department of Microbiology, IWWR, Faculty of Science, Radboud University, Nijmegen, the Netherlands

[2] Molecular Bioenergetics Group, Radboud Institute for Molecular Life Sciences, Department of Pediatrics, Radboud University Medical Center, Geert-Grooteplein Zuid 10, 6525 GA Nijmegen, the Netherlands

[3] KPA Aging-associated Diseases, CECAD Research Center, University of Cologne, Joseph-Stelzmann-Str. 26,50931 Cologne, Germany

[4] Translational Metabolic Laboratory, Department of Laboratory Medicine, Radboud University Medical Center, Geert-Grooteplein Zuid 10, 6525 GA Nijmegen, the Netherlands

[5] Microbial Physiology Group, Max Planck Institute for Marine Microbiology, Bremen, Germany.

*Corresponding authors:

Boran Kartal (bkartal@mpi-bremen.de)

Wouter Versantvoort (w.versantvoort@science.ru.nl)

Keywords: NC10, *Methylomirabilis*, Complexome profiling, Methanotrophy, Anaerobic methane oxidation, Respiratory complexes

Abstract

The atmospheric concentration of the potent greenhouse gases methane and nitrous oxide (N_2O) has increased drastically during the last century. *Methylomirabilis* bacteria can play an import role in controlling the emission of these two gases from natural ecosystems, by oxidizing methane to CO_2 and reducing nitrite to N_2 without producing N_2O. These bacteria have an anaerobic metabolism, but are proposed to possess an oxygen-dependent pathway for the activation of methane. *Methylomirabilis* bacteria reduce nitrite to NO, and are proposed to dismutate NO into O_2 and N_2 by a putative NO dismutase (NO-D). The O_2 produced in the cell can then be used for the activation of methane by a particulate methane monooxygenase. So far, the metabolic model of *Methylomirabilis* bacteria was based mainly on (meta)genomics and physiological experiments. Here we applied a complexome profiling approach to determine which of the proposed enzymes are actually expressed in *Methylomirabilis lanthanidiphila*. To validate the metabolic model, we focused on enzymes involved in respiration, and nitrogen and C1 transformation. All complexes proposed to be involved in nitrite-dependent methane oxidation, were identified in *M. lanthanidiphila*, including the putative NO-D. Furthermore, several complexes involved in nitrate reduction/ nitrite oxidation and NO reduction were detected, which likely play a role in detoxification and redox homeostasis. In conclusion, complexome profiling validated the expression and composition of enzymes proposed to be involved in the energy, methane and nitrogen metabolism of *M. lanthanidiphila,* thereby further corroborating the metabolically unique and environmentally relevant process of nitrite-dependent methane oxidation.

Introduction

Methane and nitrous oxide are potent greenhouse gases. Their emission has increased drastically since the industrial revolution due to application of synthetic nitrogenous fertilizers in agriculture [1]. Increased run-off of these fertilizers into both surface and ground waters led to an increase in nitrogen availability in the form of ammonium and nitrate resulting in water pollution and eutrophication [2, 3]. These nitrogen compounds are not only used as a nitrogen source by microorganisms, but can also be used as terminal electron acceptors in respiration. Anaerobic methane oxidation coupled to nitrate and nitrite reduction was first discovered in a microbial enrichment culture dominated by ANME-2d archaea and NC10 phylum bacteria [4]. Further studies showed that both the archaeon, *'Candidatus* Methanoperedens nitroreducens'*,* and the bacterium, *'Candidatus* Methylomirabilis oxyfera', were capable of methane oxidation independent of each other, coupling it to nitrate and nitrite reduction, respectively [5-7]. Since their discovery, *Methylomirabilis* bacteria have been detected in various ecosystems ranging from fresh water [8, 9] to marine environments [10], reviewed by Welte et al. [11].

Methylomirabilis bacteria couple the anaerobic oxidation of methane to CO_2 with the reduction of nitrite to dinitrogen gas (eq. 1). Metagenomic, transcriptomic and whole cell proteomic data combined with physiological studies on *M. oxyfera* allowed for the prediction of the metabolic model of nitrite-dependent methane oxidation [6]. This model was further supported by the analyses of the (meta)genomes of *M. limnetica* [9] and *M. lanthanidiphila* [12]. Surprisingly, these anaerobic bacteria possess the complete aerobic methane oxidation pathway, and are postulated to produce intracellular oxygen to activate methane.

$$3CH_4 + 8NO_2^- + 8H^+ = 3CO_2 + 4N_2 + 10H_2O \quad (1)$$

$$\Delta G^{o,} = -929kJ/molCH_4$$

$$2NO = N_2 + O_2 \quad (2)$$

$$\Delta G^{o,} = -173kJ/molO_2$$

Based on the genomes of *M. lanthanidiphila* and *M. oxyfera*, a metabolic model for the central energy metabolism of *Methylomirabilis* bacteria was constructed (eq. 1) [6, 12, 13]. In the proposed metabolic pathway, nitrite is first reduced to nitric oxide by cytochrome cd_1 nitrite reductase (cd_1-NIR, catalytic component encoded by NirS). Then, it is hypothesized that two molecules of nitric oxide are disproportionated to O_2 and N_2 by the putative nitric oxide dismutase (NO-D) (eq. 2) [14]. Subsequently, part of the produced O_2 is used by particulate methane monooxygenase (pMMO) to oxidize methane into methanol, and the remainder is

consumed by a terminal oxidase [15]. Methanol is oxidized by methanol dehydrogenase (MDH) either to formaldehyde [16] or directly to formate, an activity that is especially high in the lanthanide-dependent XoxF-type MDH [17]. Besides MDH, *Methylomirabilis* bacteria encode two additional dedicated systems to oxidize formaldehyde to formyl/formate: a 5,6,7,8-tetrahydromethanopterin and a 5,6,7,8-tetrahydrofolate dependent one. This formyl/formate is oxidized to CO_2 by formate dehydrogenase as the final step in methane oxidation.

Both formaldehyde and formate oxidation systems produce NADH, which can be recycled by the membrane-bound NADH dehydrogenase (NDH-1). NDH-1 couples the oxidation of NADH to the reduction of quinone and the translocation of protons. Re-oxidation of quinones is performed by the cytochrome bc_1 complex, again coupled to proton translocation. Reduced cytochrome *c* can either donate its electrons to cd_1-NIR or to a terminal oxidase [13]. Several NO reductases, which catalyze the reduction of NO to N_2O, are also present in the genome possibly preventing harmful NO concentrations and maintaining a proper redox balance [18]. The proton-motive force (*pmf)* produced by the various respiratory complexes is utilized by the F_1F_o ATP synthase to drive the production of ATP. Although *Methylomirabilis* bacteria are assumed to be unable to couple methane oxidation to nitrate reduction [5], all *Methylomirabilis* bacteria studied so far encode at least one nitrate reductase in their genome [6, 9, 12].

In addition to the oxygen-dependent methane oxidation pathway, *Methylomirabilis* bacteria are characterized by an apparent genomic redundancy in catabolic enzymes. So far, described *Methylomirabilis* species encode multiple NO reductases, two putative NO dismutases, two pathways for formaldehyde oxidation and at least two cytochrome bc_1 complex variants. The proteins involved in this model metabolic pathway are conserved in the genomes of all three available *Methylomirabilis* bacteria, although there is some variation in the apparent redundancy of the enzymes involved in various pathways. Here we use a complexome profiling approach to identify which proteins are functionally expressed in *M. lanthanidiphila* and which distinct complexes are formed. Complexome profiling has been an important tool in mitochondrial research to study the assembly and composition of respiratory complexes in both healthy and diseased cells [19-22]. Recently, this method has also been applied to study the respiratory complexes of a sulfate-reducing bacterium [23] and an anaerobic ammonium-oxidizing bacterium [24]. These studies demonstrate that complexome profiling can be a powerful tool in environmental microbiology to validate predictions inferred from (meta)genome analyses. Here, complexome profiling was applied to validate the catabolic

model of *M. lanthanidiphila* by focusing on the identification of protein complexes involved in the methane, nitrogen and energy metabolism.

Materials and methods

Enrichment culture

A 16 l (liquid volume, 10 l) *Methylomirabilis lanthanidiphila* enrichment culture (~80% enriched) was run as a continuous sequencing batch reactor (Applikon Biotechnology). The culture was originally inoculated with sediment from an Ooijpolder ditch [5]. The reactor was operated anoxically by continuous flushing of the vessel with a mixture of methane and carbon dioxide (95:5 v/v) and the medium with argon and carbon dioxide (95:5 v/v). The medium composition was: 0.649 mM $MgSO_4 \cdot 7\ H_2O$, 1.63 mM $CaCl_2 \cdot 2\ H_2O$, 0.73 mM KH_2PO_4, 0.5 µM $ZnSO_4 \cdot 7\ H_2O$, 0.25 µM $CoCl_2 \cdot 6\ H_2O$, 2.51 µM $CuSO_4$, 0.40 µM $NiCl_2 \cdot 6\ H_2O$, 0.11 µM H_3BO_3, 0.51 µM $MnCl_2 \cdot 4\ H_2O$, 0.03 µM $Na_2WO_4 \cdot 2\ H_2O$, 0.20 µM $Na_2MoO_4 \cdot 2\ H_2O$, 0.12 µM SeO_2, 0.03 µM $CeCl_3 \cdot 7\ H_2O$, and 5.4 µM $FeSO_4 \cdot 7\ H_2O$. Nitrite was added as an electron acceptor to the medium in a range of 20-40 mM, depending on the consumption rate of the culture. Concentrations of nitrite in the reactor remained below 100 µM. The temperature of the reactor was kept constant at 30 °C and the reactor was stirred at 100 rpm. Using a level sensor-controlled pump, the reactor volume was kept at 10 liters with sequential feeding and resting cycles.

Membrane preparation and solubilization

M. lanthanidiphila cells (200 ml) were harvested from the enrichment culture and centrifuged at 10,000 x g for 15 min at 4 °C. The cell pellet was resuspended in 30 ml of sample buffer, which contained 50 mM imidazole/HCl, 50 mM NaCl, 5 mM 6-aminocaproic acid, 1 mM EDTA at pH 7.0, and sonicated on ice for 8 minutes in a 5s on/ 25s off interval. After removal of the cell debris by centrifuging at 10000 x g 10 min at 4 °C, the cell-free extract was subjected to ultracentrifugation (162,000 x g, 1 hour, 4 °C). The membrane pellet was resuspended in sample buffer and diluted to a concentration of 10 mg/ml. Membrane proteins were solubilized with either n-dodecyl β-D-maltoside (DDM) or digitonin with a protein to detergent ratio of 5:2 (w/w) or 6:1 (w/w), respectively. After 5 min incubation on ice, the samples were centrifuged at 22,000 x g, 10 min, 4 °C and the supernatant containing the solubilized membrane proteins was used for Blue Native gel electrophoresis.

Blue Native gel electrophoresis and tryptic digestion

Blue Native (BN) polyacrylamide gel electrophoresis (PAGE) was performed according to Wittig et al. [25] using a 6-16% BN gradient gel (4% stacking gel). Per lane, 200 µg membrane protein sample was loaded (duplicates were run for both DDM and digitonin solubilized

samples) after the addition of glycerol to a 10% final concentration and sample additive (750 mM 6-aminocaproic acid, 5% Coomassie Brilliant Blue G-250) to a 8:1 detergent:dye ratio. Bovine heart mitochondria solubilized with either digitonin or DDM (6:1 or 3:1 w/w detergent to protein ratio, respectively) were used as molecular size markers. Gels were run at 100 V for 30 min to allow the samples to enter the separating gel. Then the voltage was increased to 400 V until the dye front reached ~1/3 of the gel. At this point, the cathode buffer B (50 mM tricine, 7.5 mM imidazole, 0.02% Coomassie blue G-250, pH 7.0) was replaced with a clear cathode buffer (50 mM tricine, 7.5 mM imidazole, pH 7.0) and the run was continued at 500 V until the dye front reached the end of the gel. After electrophoresis, the gel was washed twice with ultrapure water, fixed in 50% methanol, 10% acetic acid, 10 mM ammonium acetate for 30 minutes and stained with Coomassie blue. After washing twice with ultrapure water for 30 minutes, the lanes (two replicates each for both DDM and digitonin solubilized samples) were cut into 60 even slices of 2 mm. Each slice was diced into small pieces and transferred to a 96-well filter plate containing 150 µl of destaining solution (50% methanol, 50 mM ammonium hydrogen carbonate). In-gel digestion of the BN gel was performed according to Heide et al. [26]. Briefly, the gel pieces were washed three times for 30 minutes to remove the Coomassie dye and in between destaining solution was removed by centrifugation at 600 x g, 3 min at room temperature. To reduce disulfide bridges, the gel pieces were incubated in 120 µl 5 mM DTT for 60 minutes. After removing the DTT solution by centrifugation (600 x g, 3 min, RT) 120 µl of 15 mM chloroacetamide was added. After 45 min incubation chloroacetamide was removed by centrifugation (600 x g, 3 min, RT), and the gel pieces were dried at RT. 20 µl 5 ng/µl trypsin in 50 mM ammonium hydrogen carbonate, 1 mM $CaCl_2$ was added to the dried gel pieces, and they were incubated for 30 min at 4 °C. Then, 50 µl 50 mM ammonium hydrogen carbonate was added to cover the gel pieces, and they were incubated overnight at 37 °C. Peptides were eluted by centrifugation (600 x g, 3 min, RT) and collected in a new 96-well plate. The gel pieces were washed with 30% acetonitrile, 3% formic acid for 20 min to elute the remaining peptides. The peptide-containing solution was dried in a Concentrator Plus (Eppendorf) and peptide pellets were resuspended in 20 µl 5% acetonitrile, 0.5% formic acid.

LC-MS/MS and complexome profiling

Peptides were analyzed by liquid chromatography tandem mass spectrometry (LC-MS/MS) using a Q-Exactive mass spectrometer (Thermo Fisher Scientific) equipped with a nano-flow high-performance liquid chromatography Easy nLC-1000 system (Thermo Fisher Scientific) at the front end. LC-MS/MS parameters were set as described previously [22]. Briefly, peptides were separated in 30 minutes linear gradients of 5 to 35% acetonitrile in 0.1% formic acid using

a 100 µm ID x 150 mm length PicoTip electrospray emitter tip packed with 3 µm C18 reverse phase silica beads. The mass spectrometer was operated in a Top 20 dependent, positive ionization mode switching automatically between MS and MS/MS. Full scan MS mode (400 to 1400 m/z) operated at a resolution of 70000 with an automatic gain control (AGC) target of 1×10^6 ions and a maximum ion transfer time of 20 ms. For MS/MS fragmentation experiments the following parameters were used: resolution 17500; AGC target of 1×10^5; maximum ion transfer of 50 ms; 4.0 Th isolation window; for higher-energy collisional dissociation (HCD) a normalized collision energy of 30% was used with dynamic exclusion time of 30.0 s. A lock mass ion (*m/z*=445.12) was used for internal calibration.

Raw files were analyzed by MaxQuant software (version 1.5.0.25). Spectra were matched against the protein database of *Methylomirabilis lanthanidiphila* [12] with the addition of the sequences of known contaminants and reverse decoy with a strict FDR of 0.01% at both peptide level and protein level. In the database search, the standard mass window of 20 ppm was used for matching FTMS MS/MS peaks to theoretical ion series. Trypsin was selected as the protease allowing two missed cleavages. N-terminal acetylation and oxidation of methionine were included as dynamic modifications. Cysteine carbamidomethylation was set as fixed modification. Unique and razor peptides were considered for quantification of proteins. Migration profiles of proteins (two replicates each for both DDM and digitonin solubilized samples) were reconstructed considering their intensity-based absolute quantification (iBAQ) values and individual migration profiles were normalized on the highest intensity for each protein. Profiles were hierarchically clustered with Cluster 3.0 software by distance measures based on Pearson correlation coefficient (uncentered) using average linkage. Visualization of the interaction heatmaps was done with NOVA v0.5 [27] or Microsoft Excel. Apparent molecular masses of membrane proteins were estimated using DDM- or digitonin-solubilized oxidative phosphorylation complexes from bovine heart mitochondria as molecular mass standards. The apparent molecular masses of soluble proteins were estimated by dividing the membrane protein interpolation values by a factor of 0.8 as described previously [28].

Results and Discussion

The metabolic model of intra-aerobic methane oxidation by *Methylomirabilis* bacteria is based on (meta)genomic data combined with physiological experiments and supported by whole cell transcriptomic and proteomic studies [4, 6, 9, 12]. Here, we used complexome analyses to determine which complexes and proteins were expressed by *M. lanthanidiphila* in particular those involved in respiration as well as methane and nitrogen transformations. Isolation of the

membrane proteins with DDM or digitonin resulted in the identification and migration profile of 1002 proteins out of the 3013 possible open reading frames (Supplementary Table 1, a conversion table of "mela" loci to their respective NCBI accession number is given in Supplementary Table 2).

Nitrite reduction

Nitrite is reduced to nitric oxide in *Methylomirabilis* bacteria by a cytochrome cd_1 type nitrite reductase as the first step in their metabolism (cd_1-NIR) [6, 9, 12]. Known cd_1-NIRs are homodimers [29, 30], in the complexome, however, cd_1-NIR (mela_0586) migrated predominantly at its monomer size (60 kDa) (Figure 1). As the heme to heme distances between *c*-hemes of the monomer subunits are too long for efficient electron transfer and each subunit functions independently [31], the formation of a dimer might not be necessary for a functional enzyme and in *M. lanthanidiphila* cd_1-NIR might thus be present as a monomer. However, since a small amount was detected as a dimer, it is most likely that the association of the monomers in *M. lanthanidiphila* is fragile and is mostly disrupted during the experimental procedures.

Nitric oxide dismutation

A unique feature of *Methylomirabilis* bacteria is the hypothesized intracellular oxygen production for methane oxidation. Here, two molecules of nitric oxide are proposed to be dismutated into molecular oxygen and dinitrogen gas by a putative NO dismutase enzyme (eq. 2) [14]. This reaction is thermodynamically feasible, but the complex bond rearrangements make this most likely the rate-limiting step in the metabolism of *Methylomirabilis* [11]. Two candidate enzymes (NO-D1 and NO-D2) that might perform this oxygenic reaction have been identified [6]. These putative NO-Ds are homologous to the respiratory quinol-dependent nitric oxide reductases, but have amino acid substitutions in the catalytic site, quinol binding site and proton channel [14]. These amino acid substitutions are conserved in the NO-D sequences of both *M. limnetica* [9] and *M. lanthanidiphila* [12], which suggests that NO-Ds have a different catalytic center, and cannot accept external electrons and H^+ from outside the protein [14]. These amino acid substitutions would likely impede NO reduction to N_2O, but could facilitate their role as NO dismutases.

In the complexome, the abundance of NO-D2 (mela_2434), as estimated by the total intensity based absolute quantification (iBAQ) values, was in the same order of magnitude as cd_1-NIR (mela_0586), amongst the top 20 most abundant proteins, whereas NO-D1 (mela_2433) was about 25-fold less abundant, in line with previously performed transcriptome experiments [6, 32]. The complexome profiling showed the migration of NO-D2 predominantly as a dimer in

the DDM sample, whilst a small fraction was present at the monomer size (Figure 1). In the digitonin sample NO-D2 migrated predominantly at a trimer size, although a small fraction was still detected at the dimer size. NO-D1 (mela_2433) had a similar profile as NO-D2 in the DDM sample, but was apparently dissociated in the digitonin sample. Only a minor fraction of NO-D1 was found at the dimer size and the majority was detected at ~50 kDa, even below the size of a monomer (~90 kDa) (Figure 1). This could either be due to degradation of NO-D1, or because of a less reliable estimation of the apparent mass from the Blue-Native gel electrophoresis due to lack of complexes suitable for calibration in the lower mass range. Since NO-D1 was found to migrate differently from NO-D2 in the digitonin sample it could be concluded that both isoforms of NO dismutase form homodimers/trimers. The formation of functional dimers has also been reported for the closely related cytochrome *c*-dependent nitric oxide reductase [33]. Although the high abundance of the putative NO-Ds in the complexome indicates an importance for the metabolism of *Methylomirabilis* bacteria, their role as NO dismutases remains hypothetical. Rigorous characterization of these enzymes is necessary to shed light on their role within the metabolism of *Methylomirabilis* species as well as other microorganisms, such as gammaproteobacterial HdN1, the flavobacterium *Muricauda ruestringensis* and the eukaryortic foraminifera species *Globobulimina*, which encode NO-D like enzymes [14, 34].

Nitric oxide reduction

Besides the proposed potential to dismutate nitric oxide, *M. lanthanidiphila* encodes for a canonical quinol-dependent nitric oxide reductase (qNOR, mela_00936) and two proteins belonging to novel NOR types: an sNOR (mela_02377-2378) and a gNOR (mela_02626-2627) [12, 18, 35]. Of these NORs, the qNOR was detected migrating solely as a dimer (Figure 1). For the sNOR, only subunit II (mela_2377) was identified in the complexome, migrating as both a monomer and dimer complex in the DDM and mainly as a dimer complex in the digitonin sample (Figure 1). The observation of sNOR subunit II at the monomer and dimer complex size strongly suggested the presence of the entire complex. Based on their iBAQ values, both qNOR and sNOR subunit II appear about ~300 and 500 times less abundant than NO-D2, respectively, and were most likely involved in the detoxification of nitric oxide, to prevent nitrosative stress [18]. Quinol functions as electron donor for qNOR [36], whereas cytochrome *c* is the electron donor for sNOR [37]. By expressing both q- and sNOR, *M. lanthanidiphila* could tap into two different electron pools to prevent NO accumulation. In addition, both sNOR and qNOR are electrogenic enzymes [37, 38], so besides avoiding toxic NO levels, NO reduction might contribute to the maintenance of a *pmf*, thereby linking NO detoxification to ATP production.

Nitrate reduction

Nitrate-dependent methane oxidation by *Methylomirabilis* bacteria is suggested to be unfeasible due to a redox imbalance [18], and accordingly *M. oxyfera* has been shown incapable of nitrate reduction with methane as the electron donor under tested growth and experimental conditions [5]. Still, the genome of *M. lanthanidiphila* encodes for one periplasmic NapAB (mela_00582-583) and two membrane-bound Nar-type nitrate reductases (mela_00628-630 & mela_2381-2385) [12]. Surprisingly, all three nitrate reductases were detected in the complexome (Figure 1). NapA migrated to 120 kDa in the gel, the expected size of a functional NapAB heterodimer (100 kDa), even though the small NapB subunit was not detected in the gel. Furthermore, the first *nar* cluster (mela_00628-630), of which the NarG contains a TAT signal for translocation of the mature protein to the periplasm, was detected at the expected size of a NarGH-1complex (mela_00628-9; 170 kDa), indicating that NarGH might have dissociated from the membrane-associated NarI-1 subunit during the experimental procedures. Unaltered migration between both DDM and digitonin samples supported the dissociation of NarGH from NarI, since its migration was unaffected by the type of detergent applied. The second *nar* cluster (mela_02381-2385) did not contain a TAT signal and thus would stay oriented to the cytoplasm. Here, NarG (mela_02381) and NarH (mela_02383) seemed to co-migrate, but the size they were detected at matched neither the NarGH-2 (200 kDa) nor the NarGHI-2 complex (225 kDa). Both subunits were predominantly detected at 150 kDa in the DDM sample, the size of the NarG2 subunit, indicating dissociation of the complex. In the digitonin sample both subunits were detected predominantly at the top of the gel, indicating they were probably insufficiently solubilized in this detergent. All three nitrate reductases were, however, not very abundant in the complexome, with total iBAQ values of roughly 120, 160 and 650 times lower than the cd_1-NIR for NapA, NarG1 and NarG2, respectively.

The role these enzymes play in the metabolism of *M. lanthanidiphila* remains unknown. The enrichment culture was not fed with nitrate and the nitrate concentration stayed below the detection level (~80 μM). Still, three systems to reduce nitrate to nitrite were detected in the complexome, albeit in low abundance. These systems might be induced by the presence of nitrite, as has been shown for both NAP and NAR of *E. coli* [39]. They might have a role in balancing the redox state in the cell by shuttling electrons on nitrate, although this nitrate has to be produced first, since it is not added externally to the bioreactor. The NarGH-2 might also function as a nitrite oxidoreductase (NXR), as the NarGHI-2 gene cluster (mela_02381-2385) is closely related to the NXR of nitrite oxidizers including anaerobic ammonium-oxidizing (anammox) bacteria [12]. Many aerobic and anaerobic nitrite-oxidizing bacteria such as

Nitrotoga fabula, *N. moscoviensis* and *K. stuttgartiensis* encode NXRs that are bidirectional, i.e. these microorganisms has been shown to be capable of reducing nitrate using the same protein complex [40-42] and as such their function is dependent on the presence of substrate (either nitrate or nitrite) and alternative electron donors or acceptors. Therefore, it cannot be predicted from sequence analyses whether they function as nitrite-oxidizing or nitrate-reducing protein complexes. Combined, these NAP and NAR/NXR systems in *M. lanthanidiphila* might work together to either provide or consume electrons, depending on the redox state of the cell. Furthermore, they could enable these microorganisms to grow on nitrate reduction or nitrite oxidation, depending on the availability of these substrates. However, currently there is no experimental evidence to support either of these functions.

Methane oxidation

Methane is oxidized in *M. lanthanidiphila* by the membrane-bound copper-dependent particulate methane mono-oxygenase (pMMO). Due to the hydrophobic nature of methane, it is calculated to partition in the membrane bilayer at a molar ratio of ~10:1 [43], increasing its effective concentration accessible for pMMO. This enzyme consists of three subunits: pmoB (mela_02441), pmoA (mela_02442) and pmoC (mela_03065), which form a functional $\alpha_3\beta_3\gamma_3$ homotrimer [44] and oxidize methane to methanol. All three pMMO subunits were identified comigrating predominantly as a $\alpha_3\beta_3\gamma_3$ homotrimer in the DDM and a $\alpha_4\beta_4\gamma_4$ homotetramer in the digitonin sample (Figure 2). Both DDM and digitonin profiles also showed a small population migrating at higher apparent molecular mass, fitting with $(\alpha_3\beta_3\gamma_3)_2$ and $(\alpha_3\beta_3\gamma_3)_4$ stoichiometries for DDM, and $(\alpha_4\beta_4\gamma_4)_2$ and $(\alpha_4\beta_4\gamma_4)_4$ stoichiometries for digitonin.

Methanol oxidation

Methanol is oxidized in *M. lanthandiphila* by an XoxF-type MDH (mela_00916; [12]. These XoxF-type MDHs were shown to be homodimeric enzymes, binding lanthanides in their active site [17] in contrast to their calcium binding heterotetrameric MxaFI counterpart [45]. XoxF was found smeared throughout the gel (Figure 2), with the majority migrating at very high molecular mass, indicating a large oligomeric state far above the functional dimer. This might be due to aggregation of MDH which was also observed during the purification of *M. fumariolicum* MDH, when the buffers were not supplemented with methanol [17]. XoxF has been shown to readily oxidize not only methanol but also formaldehyde [17].

Formaldehyde oxidation

Besides the XoxF-type MDH, *M. lanthanidiphila* encodes for two additional systems to oxidize formaldehyde: one 5,6,7,8-tetrahydromethanopterin (H_4MPT) and one 5,6,7,8-tetrahydrofolate

(H_4F) dependent protein [12]. FAE, MTD and MCH (Fae, mela_2741; Mtd, mela_2742; Mch, mela_2748), the three enzymes responsible for the sequential formation of 5-formyl-H_4MPT were all identified in the complexome. FAE migrated dominantly to 60 kDa in the DDM sample (Figure 2), similar to the expected mass shown for the homopentameric conformation in *M. extorquens* [46]. In addition, a population was shown to migrate at an apparent mass of 120 kDa, indicating a decamer formation. MCH are reported either as homodimeric [47, 48] or homotrimeric enzymes [49-51]. In *M. lanthanidiphila* however, MCH was predominantly detected at its monomer size (30 kDa), suggesting that its quaternary structure was disrupted during sample preparation. MTD from *Methylomirabilis* has been proposed to couple either 5,10-methylene-H_4MPT or 5,10-methylene-H_4F oxidation to reduction of $NAD(P)^+$ to sustain both catabolic and anabolic reactions [18]. *M. lanthanidiphila* MTD migrated mainly at its monomer size (30 kDa), but a small part was detected in tetrameric conformation (120 kDa, Figure 2), which is distinct from the homotrimeric MtdA [52] and homohexameric MtdB [53]. Phylogenetically *Methylomirabilis* Mtd clusters between MtdA and MtdB [54] and it thus also seems to adopt a different quaternary structure. The presence of a dedicated formaldehyde oxidation system in the proteome of *M. lanthanidiphila* indicated that at least some, if not all the methanol would be converted into formaldehyde instead of formate by the XoxF-type MDH. Therefore, unlike the verrucomicrobial *M. fumariolicum*, *M. lanthanidiphila* might not necessarily skip free formaldehyde as an intermediate in methane oxidation [17, 55].

Formate/ formyl oxidation

Methylomirabilis species possess a unique formyl oxidation system, comprising of the four-subunit 5-formyl-H_4MPT:methanofuran formyltransferase system (FhcBADC, mela_2743-47) known from aerobic methylotrophs [56] with an additional FwdD subunit [9, 12, 18]. Furthermore, the FhcB subunit shares homology with the archaeal FwdB, including the residues required for binding a 4Fe-4S cluster and a pterin cofactor, indicating a possible function as formylmethanofuran dehydrogenase (Reimann et al., 2015). In *M. lanthanidiphila* this complex was detected as a FwdDFhcBADC dimer and as a FwdDFhcBAC monomer (Figure 2). The loss of the FhcD subunit and subsequent loss of dimer formation has also been observed in *M. extorquens* [57].

Besides the aforementioned formyl transferase/ hydrolase system, *M. lanthanidiphila* possesses another formate oxidation system consisting of FdhA (mela_1504) and FdhB (mela_1503) [12]. These proteins migrated predominantly as a heterodimer (Figure 2).

RuBisCo

In contrast to the characterized proteobacterial methanotrophs, *Methylomirabilis* bacteria are autotrophic and employ the Calvin-Benson-Bassham (CBB) cycle for CO_2 fixation [58]. The first step in carbon fixation via the CBB cycle is the carboxylation of ribulose-1,5-bisphosphate catalyzed by the RuBisCo enzyme. There are four forms of the enzyme found in nature (I, II, III and IV) [59] and phylogenetic analysis of the large RuBisCo subunit of *M. oxyfera* classified it as type Ic [58]. Form I RuBisCos are octameric complexes consisting of a catalytic core of 8 large subunits, with 8 small subunits lining the top and bottom of the core [60]. In *M. lanthanidiphila* the RuBisCo complex migrated at 560 kDa in the DDM sample (Figure 2), which was in agreement with the expected size of a L_8S_8 octameric complex (560 kDa). In the digitonin sample, the CbbL was found to be smeared throughout the gel and did not seem to comigrate with CbbS, which is most likely due to dissociation by the applied detergent.

NADH dehydrogenase

In *M. lanthanidiphila* NADH is (re)generated by the oxidation of formaldehyde and formate, which can be recycled by an NADH dehydrogenase (NDH-1) and thereby fuel respiration. All NDH subunits are encoded twice in the genome of *M. lanthanidiphila*, with the exception of the NADH oxidizing N-module (NdhE, NdhF and NdhG), which is only present as a single copy [12]. In the complexome, all NDH-1(1) subunits except NdhJ (mela_0376), NdhK (mela_0377) and NdhE (mela_0387) were detected (Figure 3). However, a complete NDH complex (complex I) could not be detected. For example, NDH-1 seemed to be partially dissociated. Subunits NdhA, NdhC, NdhD, NdhH, NdhM, NdhN, NdhI, NdhB comigrated to approximately 290 kDa in the DDM treated sample, which was in line with the combined masses of these subunits. In the digitonin treated sample the majority of the subunits migrated to 750 kDa, which was too large for just the complete NDH-1(1) complex (490 kDa, or 450 kDa with the missing NdhJ, NdhK and NdhE subunits) and implied the comigration with another protein complex. However, no apparent complexes were found to comigrate with NDH-1(1) in the digitonin sample. Of the second NADH dehydrogenase (NDH-1(2)) only NdhD and NdhJ were detected, which migrated together with the NdhF subunit of NDH-1(1) in the DDM sample at 600 kDa, but did not clearly comigrate in the digitonin treated sample.

Cytochrome bc_1 *complexes*

Cytochrome bc_1 complexes couple the oxidation of quinols to the reduction of cytochrome *c* and contribute to the maintenance of the *pmf* via a unique mechanism called the proton-motive

Q-cycle [61]. Most organisms contain at least one version of the cytochrome bc_1 complex, since it can be inserted into any respiratory chain operating with quinones that has a sufficient redox span for the turnover of three enzymes [62]. Some organisms, including *M. lanthanidiphila,* encode for multiple cytochrome bc_1 complexes. Although most organisms containing multiple versions are poorly studied, dedicated roles under different growth conditions or a bias in forward or reverse electron transfer has been proposed [63]. In the anammox bacterium *Kuenenia stuttgartiensis* complexome profiling showed that two different cytochrome bc_1 complexes were present under standard laboratory growth conditions. Both complexes were speculated to perform dedicated roles in anammox energy metabolism [24]. The genome of *M. lanthanidiphila* encodes for a cytochrome bc_1 complex containing a nonaheme *c* subunit (mela_01529-01531) and a complex containing an octaheme *c* subunit (mela_01456-01459). Of the former complex, only the nonaheme *c* subunit is detected, which did not migrate as a focused band. The latter complex has a b_6f-like architecture with a split cytochrome *b* subunit and a conserved cysteine residue proposed to be involved in the binding of heme c_i [63]. In the complexome this complex was identified at a size of ~560 kDa, the additional membrane spanning subunit IV however was not detected (Figure 4). Still, the migration of the three other subunits at such a high molecular mass indicated the presence of a complete cytochrome bc_1 complex. The observed apparent mass of 560 kDa was too large for the commonly observed dimer (~360 kDa), but would fit the size of a supercomplex of dimeric cytochrome bc_1 complex with a terminal oxidase dimer (~580 kDa), a supercomplex which has been observed in mitochondria [64] and various aerobic prokaryotes [65, 66]. A high resolution structure of this supercomplex from *Mycobacterium smegmatis* was recently reported [67]. However, no terminal oxidase subunits were detected comigrating with the cytochrome bc_1 complex subunits.

Terminal oxidase

Methylomirabilis bacteria couple the oxidation of methane to the reduction of nitrite in a 3:8 stoichiometry (eq. 1). The eight molecules of nitrite produce four molecules of oxygen, whereas only three are consumed in the oxidation of methane. This leaves four electrons and one oxygen molecule, which can be consumed by a terminal oxidase proposed to be a quinol-dependent bo_3-type oxidase [15]. Reevaluation of the sequence of this bo_3-type oxidase revealed that it belonged to a novel clade of nitric oxide reductases: gNOR (mela_02626-2627; [18], although a function as an O_2 reductase cannot be excluded. However, no subunits of the gNOR were detected in the membrane complexome. The only HCO in *M. lanthanidiphila* that can be reliably annotated as an O_2 reductase is an aa_3-type cytochrome *c* oxidase (mela_00198-200).

All three subunits of this oxidase co-migrated at a size of 150 kDa in the DDM sample and 200 kDa in the digitonin sample, respectively (Figure 4). For the digitonin sample, this indicated the formation of a dimer, whereas in the DDM sample the apparent mass was ranged in the middle between a monomer and dimer formation. Regardless of the oligomeric state, this indicated that *M. lanthanidiphila* could employ the low affinity, high efficiency aa_3-type oxidase to respire the surplus oxygen. This oxidase however is usually expressed under high oxygen concentrations. Its lower affinity for oxygen would make it a less efficient competitor for the pMMO for oxygen, ensuring sufficient turnover of methane. Alternatively, the internally produced oxygen in the membrane of *M. lanthanidiphila* might provide a high enough local oxygen concentration to effectively feed the oxidase.

ATP synthase

M. lanthanidiphila encodes for a single F-type ATP synthase to harvest the *pmf* and form ATP. All detected subunits migrated at ~700 kDa, apart from the membrane-embedded AtpB (mela_00382) subunit (Figure 4), which was not detected. Although not all subunits were detected, the apparent mass of the detected complex indicated the presence of a fully assembled ATP synthase (620-690 kDa, depending on the number of c subunits). The number of c subunits in the bacterial ATP synthase can vary between 9-15 [68, 69].

Conclusions

Here the complexome of *M. lanthanidiphila* was examined for protein complexes involved in respiration, methane, C1 and nitrogen transformations. All protein complexes that were proposed to be involved in the anaerobic, oxygen-dependent oxidation of methane coupled to nitrite reduction were identified in the complexome, including the two putative NO-Ds (Figure 5). Remarkably, three protein complexes potentially involved in nitrate reduction were identified, one periplasmic nitrate reductase (NAP) and two membrane-bound nitrate reductases/ nitrite oxidoreductases (NAR/NXR). The role of these proteins remained unknown, since neither nitrite oxidation to nitrate nor nitrate-dependent methane oxidation by any *Methylomirabilis* species has so far been shown. Furthermore, two nitric oxide reductases (qNOR and sNOR) were present in the complexome, which might be involved in NO detoxification and intracellular redox balance. Finally, the unique formyl oxidation system, including an FwdD subunit was identified. All in all, the (meta)genomic-based model was validated on a complexome level. The next step would be the physiological and biochemical characterization of the energy metabolism, by purifying and characterizing the relevant enzymes, such as the enigmatic NO-D.

Acknowledgements

The authors would like to thank Olivia Rasigraf for supplying biomass. WV, JR and MSMJ were supported by the European Research Council [ERC AG Ecomom 339880]. WV was supported by the Netherlands Organization for Scientific Research [NWO 824.15.011 to BK]. BK was supported by the European Research Council [ERC 640422].

References

[1] IPCC, Climate Change 2014: Synthesis report. Contribution of working groups i, ii and iii to the fifth assessment report of the intergovernmental panel on climate change., IPCC, Place Published, 2014.

[2] J.N. Galloway, A.R. Townsend, J.W. Erisman, M. Bekunda, Z. Cai, J.R. Freney, L.A. Martinelli, S.P. Seitzinger, M.A. Sutton, Transformation of the Nitrogen Cycle: Recent Trends, Questions, and Potential Solutions, Science, 320 (2008) 889-892.

[3] J.N. Galloway, F.J. Dentener, D.G. Capone, E.W. Boyer, R.W. Howarth, S.P. Seitzinger, G.P. Asner, C.C. Cleveland, P.A. Green, E.A. Holland, D.M. Karl, A.F. Michaels, J.H. Porter, A.R. Townsend, C.J. Vöosmarty, Nitrogen Cycles: Past, Present, and Future, Biogeochemistry, 70 (2004) 153-226.

[4] A.A. Raghoebarsing, A. Pol, K.T. van de Pas-Schoonen, A.J. Smolders, K.F. Ettwig, W.I. Rijpstra, S. Schouten, J.S. Damste, H.J. Op den Camp, M.S. Jetten, M. Strous, A microbial consortium couples anaerobic methane oxidation to denitrification, Nature, 440 (2006) 918-921.

[5] K.F. Ettwig, S. Shima, K.T. van de Pas-Schoonen, J. Kahnt, M.H. Medema, H.J. Op den Camp, M.S. Jetten, M. Strous, Denitrifying bacteria anaerobically oxidize methane in the absence of Archaea, Environ Microbiol, 10 (2008) 3164-3173.

[6] K.F. Ettwig, M.K. Butler, D. Le Paslier, E. Pelletier, S. Mangenot, M.M. Kuypers, F. Schreiber, B.E. Dutilh, J. Zedelius, D. de Beer, J. Gloerich, H.J. Wessels, T. van Alen, F.

513 Luesken, M.L. Wu, K.T. van de Pas-Schoonen, H.J. Op den Camp, E.M. Janssen-Megens,
514 K.J. Francoijs, H. Stunnenberg, J. Weissenbach, M.S. Jetten, M. Strous, Nitrite-driven
515 anaerobic methane oxidation by oxygenic bacteria, Nature, 464 (2010) 543-548.
516 [7] M.F. Haroon, S. Hu, Y. Shi, M. Imelfort, J. Keller, P. Hugenholtz, Z. Yuan, G.W. Tyson,
517 Anaerobic oxidation of methane coupled to nitrate reduction in a novel archaeal lineage,
518 Nature, 500 (2013) 567-570.
519 [8] K.F. Ettwig, T. van Alen, K.T. van de Pas-Schoonen, M.S. Jetten, M. Strous, Enrichment
520 and molecular detection of denitrifying methanotrophic bacteria of the NC10 phylum, Appl
521 Environ Microbiol, 75 (2009) 3656-3662.
522 [9] J.S. Graf, M.J. Mayr, H.K. Marchant, D. Tienken, P.F. Hach, A. Brand, C.J. Schubert,
523 M.M.M. Kuypers, J. Milucka, Bloom of a denitrifying methanotroph, 'Candidatus
524 Methylomirabilis limnetica', in a deep stratified lake, Environ Microbiol, 20 (2018) 2598-
525 2614.
526 [10] Z. He, S. Geng, C. Cai, S. Liu, Y. Liu, Y. Pan, L. Lou, P. Zheng, X. Xu, B. Hu,
527 Anaerobic Oxidation of Methane Coupled to Nitrite Reduction by Halophilic Marine NC10
528 Bacteria, Appl Environ Microbiol, 81 (2015) 5538-5545.
529 [11] C.U. Welte, O. Rasigraf, A. Vaksmaa, W. Versantvoort, A. Arshad, H.J. Op den Camp,
530 M.S. Jetten, C. Luke, J. Reimann, Nitrate- and nitrite-dependent anaerobic oxidation of
531 methane, Environ Microbiol Rep, 8 (2016) 941-955.
532 [12] W. Versantvoort, S. Guerrero-Cruz, D.R. Speth, J. Frank, L. Gambelli, G. Cremers, T.
533 van Alen, M.S.M. Jetten, B. Kartal, H.J.M. Op den Camp, J. Reimann, Comparative
534 Genomics of Candidatus Methylomirabilis Species and Description of Ca. Methylomirabilis
535 Lanthanidiphila, Front Microbiol, 9 (2018) 1672.
536 [13] M.L. Wu, K.F. Ettwig, M.S. Jetten, M. Strous, J.T. Keltjens, L. van Niftrik, A new intra-
537 aerobic metabolism in the nitrite-dependent anaerobic methane-oxidizing bacterium
538 Candidatus 'Methylomirabilis oxyfera', Biochem Soc Trans, 39 (2011) 243-248.

[14] K.F. Ettwig, D.R. Speth, J. Reimann, M.L. Wu, M.S. Jetten, J.T. Keltjens, Bacterial oxygen production in the dark, Front Microbiol, 3 (2012) 273.

[15] M.L. Wu, S. de Vries, T.A. van Alen, M.K. Butler, H.J. Op den Camp, J.T. Keltjens, M.S. Jetten, M. Strous, Physiological role of the respiratory quinol oxidase in the anaerobic nitrite-reducing methanotroph 'Candidatus Methylomirabilis oxyfera', Microbiology, 157 (2011) 890-898.

[16] C. Anthony, The structure of bacterial quinoprotein dehydrogenases, Int J Biochem, 24 (1992) 29-39.

[17] A. Pol, T.R. Barends, A. Dietl, A.F. Khadem, J. Eygensteyn, M.S. Jetten, H.J. Op den Camp, Rare earth metals are essential for methanotrophic life in volcanic mudpots, Environ Microbiol, 16 (2014) 255-264.

[18] J. Reimann, M.S.M. Jetten, J.T. Keltjens, Metal Enzymes in “Impossible” Microorganisms Catalyzing the Anaerobic Oxidation of Ammonium and Methane, in: P.M.H. Kroneck, M.E. Sosa Torres (Eds.) Sustaining Life on Planet Earth: Metalloenzymes Mastering Dioxygen and Other Chewy Gases, Springer International Publishing, Place Published, 2015, pp. 257-313.

[19] M.A. Huynen, M. Muhlmeister, K. Gotthardt, S. Guerrero-Castillo, U. Brandt, Evolution and structural organization of the mitochondrial contact site (MICOS) complex and the mitochondrial intermembrane space bridging (MIB) complex, Biochim Biophys Acta, 1863 (2016) 91-101.

[20] T. Konig, S.E. Troder, K. Bakka, A. Korwitz, R. Richter-Dennerlein, P.A. Lampe, M. Patron, M. Muhlmeister, S. Guerrero-Castillo, U. Brandt, T. Decker, I. Lauria, A. Paggio, R. Rizzuto, E.I. Rugarli, D. De Stefani, T. Langer, The m-AAA Protease Associated with Neurodegeneration Limits MCU Activity in Mitochondria, Molecular cell, 64 (2016) 148-162.

564 [21] L. Sanchez-Caballero, B. Ruzzenente, L. Bianchi, Z. Assouline, G. Barcia, M.D.
565 Metodiev, M. Rio, B. Funalot, M.A. van den Brand, S. Guerrero-Castillo, J.P. Molenaar, D.
566 Koolen, U. Brandt, R.J. Rodenburg, L.G. Nijtmans, A. Rotig, Mutations in Complex I
567 Assembly Factor TMEM126B Result in Muscle Weakness and Isolated Complex I
568 Deficiency, American journal of human genetics, 99 (2016) 208-216.
569 [22] S. Guerrero-Castillo, F. Baertling, D. Kownatzki, H.J. Wessels, S. Arnold, U. Brandt, L.
570 Nijtmans, The Assembly Pathway of Mitochondrial Respiratory Chain Complex I, Cell
571 Metab, 25 (2017) 128-139.
572 [23] L. Wöhlbrand, H.S. Ruppersberg, C. Feenders, B. Blasius, H.P. Braun, R. Rabus,
573 Analysis of membrane-protein complexes of the marine sulfate reducer Desulfobacula
574 toluolica Tol2 by 1D blue native-PAGE complexome profiling and 2D blue native-/SDS-
575 PAGE, Proteomics, 16 (2016) 973-988.
576 [24] N.M. de Almeida, H.J. Wessels, R.M. de Graaf, C. Ferousi, M.S. Jetten, J.T. Keltjens, B.
577 Kartal, Membrane-bound electron transport systems of an anammox bacterium: A
578 complexome analysis, Biochim Biophys Acta, 1857 (2016) 1694-1704.
579 [25] I. Wittig, H.P. Braun, H. Schagger, Blue native PAGE, Nat Protoc, 1 (2006) 418-428.
580 [26] H. Heide, L. Bleier, M. Steger, J. Ackermann, S. Drose, B. Schwamb, M. Zornig, A.S.
581 Reichert, I. Koch, I. Wittig, U. Brandt, Complexome profiling identifies TMEM126B as a
582 component of the mitochondrial complex I assembly complex, Cell Metab, 16 (2012) 538-
583 549.
584 [27] H. Giese, J. Ackermann, H. Heide, L. Bleier, S. Drose, I. Wittig, U. Brandt, I. Koch,
585 NOVA: a software to analyze complexome profiling data, Bioinformatics (Oxford, England),
586 31 (2015) 440-441.
587 [28] I. Wittig, T. Beckhaus, Z. Wumaier, M. Karas, H. Schagger, Mass estimation of native
588 proteins by blue native electrophoresis: principles and practical hints, Mol Cell Proteomics, 9
589 (2010) 2149-2161.

590 [29] S.C. Baker, N.F.W. Saunders, A.C. Willis, S.J. Ferguson, J. Hajdu, V. Fülöp,
591 Cytochrome cd1 Structure: unusual haem environments in a nitrite reductase and analysis of
592 factors contributing to β-propeller folds11Edited by K. Nagai, Journal of Molecular Biology,
593 269 (1997) 440-455.
594 [30] D. Nurizzo, M.-C. Silvestrini, M. Mathieu, F. Cutruzzolà, D. Bourgeois, V. Fülöp, J.
595 Hajdu, M. Brunori, M. Tegoni, C. Cambillau, N-terminal arm exchange is observed in the
596 2.15 Å crystal structure of oxidized nitrite reductase from Pseudomonas aeruginosa,
597 Structure, 5 (1997) 1157-1171.
598 [31] B.A. Averill, Dissimilatory Nitrite and Nitric Oxide Reductases, Chem Rev, 96 (1996)
599 2951-2964.
600 [32] F.A. Luesken, M.L. Wu, H.J. Op den Camp, J.T. Keltjens, H. Stunnenberg, K.J.
601 Francoijs, M. Strous, M.S. Jetten, Effect of oxygen on the anaerobic methanotroph
602 'Candidatus Methylomirabilis oxyfera': kinetic and transcriptional analysis, Environ
603 Microbiol, 14 (2012) 1024-1034.
604 [33] J. Hendriks, A. Warne, U. Gohlke, T. Haltia, C. Ludovici, M. Lubben, M. Saraste, The
605 active site of the bacterial nitric oxide reductase is a dinuclear iron center, Biochemistry, 37
606 (1998) 13102-13109.
607 [34] C. Woehle, A.S. Roy, N. Glock, T. Wein, J. Weissenbach, P. Rosenstiel, C. Hiebenthal,
608 J. Michels, J. Schonfeld, T. Dagan, A Novel Eukaryotic Denitrification Pathway in
609 Foraminifera, Curr Biol, 28 (2018) 2536-2543 e2535.
610 [35] J. Hemp, R.B. Gennis, Diversity of the Heme–Copper Superfamily in Archaea: Insights
611 from Genomicsand Structural Modeling, in: G. Schäfer, H.S. Penefsky (Eds.) Bioenergetics:
612 Energy Conservation and Conversion, Springer Berlin Heidelberg, Place Published, 2008, pp.
613 1-31.
614 [36] T. Tosha, Y. Shiro, Crystal structures of nitric oxide reductases provide key insights into
615 functional conversion of respiratory enzymes, IUBMB Life, 65 (2013) 217-226.

[37] S. Al-Attar, S. de Vries, An electrogenic nitric oxide reductase, FEBS Lett, 589 (2015) 2050-2057.

[38] N. Gonska, D. Young, R. Yuki, T. Okamoto, T. Hisano, S. Antonyuk, S.S. Hasnain, K. Muramoto, Y. Shiro, T. Tosha, P. Ädelroth, Characterization of the quinol-dependent nitric oxide reductase from the pathogen Neisseria meningitidis, an electrogenic enzyme, Scientific Reports, 8 (2018) 3637.

[39] H. Wang, C.-P. Tseng, R.P. Gunsalus, The napF and narG Nitrate Reductase Operons in Escherichia coli Are Differentially Expressed in Response to Submicromolar Concentrations of Nitrate but Not Nitrite, Journal of Bacteriology, 181 (1999) 5303-5308.

[40] H. Koch, S. Lücker, M. Albertsen, K. Kitzinger, C. Herbold, E. Spieck, P.H. Nielsen, M. Wagner, H. Daims, Expanded metabolic versatility of ubiquitous nitrite-oxidizing bacteria from the genus Nitrospira, Proceedings of the National Academy of Sciences, 112 (2015) 11371-11376.

[41] B. Kartal, M.M.M. Kuypers, G. Lavik, J. Schalk, H.J.M. Op den Camp, M.S.M. Jetten, M. Strous, Anammox bacteria disguised as denitrifiers: nitrate reduction to dinitrogen gas via nitrite and ammonium, Environmental Microbiology, 9 (2007) 635-642.

[42] K. Kitzinger, H. Koch, S. Lucker, C.J. Sedlacek, C. Herbold, J. Schwarz, A. Daebeler, A.J. Mueller, M. Lukumbuzya, S. Romano, N. Leisch, S.M. Karst, R. Kirkegaard, M. Albertsen, P.H. Nielsen, M. Wagner, H. Daims, Characterization of the First "Candidatus Nitrotoga" Isolate Reveals Metabolic Versatility and Separate Evolution of Widespread Nitrite-Oxidizing Bacteria, MBio, 9 (2018).

[43] K.W. Miller, L. Hammond, E.G. Porter, The solubility of hydrocarbon gases in lipid bilayers, Chemistry and Physics of Lipids, 20 (1977) 229-241.

[44] R.L. Lieberman, A.C. Rosenzweig, Crystal structure of a membrane-bound metalloenzyme that catalyses the biological oxidation of methane, Nature, 434 (2005) 177.

642 [45] C. Anthony, Methanol Dehydrogenase, a PQQ-Containing Quinoprotein Dehydrogenase,
643 in: A. Holzenburg, N.S. Scrutton (Eds.) Enzyme-Catalyzed Electron and Radical Transfer:
644 Subcellular Biochemistry, Springer US, Place Published, 2000, pp. 73-117.
645 [46] P. Acharya, M. Goenrich, C.H. Hagemeier, U. Demmer, J.A. Vorholt, R.K. Thauer, U.
646 Ermler, How an enzyme binds the C1 carrier tetrahydromethanopterin. Structure of the
647 tetrahydromethanopterin-dependent formaldehyde-activating enzyme (Fae) from
648 Methylobacterium extorquens AM1, J Biol Chem, 280 (2005) 13712-13719.
649 [47] A.R. Klein, J. Breitung, D. Linder, K.O. Stetter, R.K. Thauer, N-5, N-10-
650 Methenyltetrahydromethanopterin Cyclohydrolase from the Extremely Thermophilic Sulfate
651 Reducing Archaeoglobus-Fulgidus - Comparison of Its Properties with Those of the
652 Cyclohydrolase from the Extremely Thermophilic Methanopyrus-Kandleri, Archives of
653 Microbiology, 159 (1993) 213-219.
654 [48] B.K. Pomper, J.A. Vorholt, L. Chistoserdova, M.E. Lidstrom, R.K. Thauer, A methenyl
655 tetrahydromethanopterin cyclohydrolase and a methenyl tetrahydrofolate cyclohydrolase in
656 Methylobacterium extorquens AM1, Eur J Biochem, 261 (1999) 475-480.
657 [49] W. Grabarse, M. Vaupel, J.A. Vorholt, S. Shima, R.K. Thauer, A. Wittershagen, G.
658 Bourenkov, H.D. Bartunik, U. Ermler, The crystal structure of
659 methenyltetrahydromethanopterin cyclohydrolase from the hyperthermophilic archaeon
660 Methanopyrus kandleri, Structure, 7 (1999) 1257-1268.
661 [50] V. Upadhyay, U. Demmer, E. Warkentin, J. Moll, S. Shima, U. Ermler, Structure and
662 catalytic mechanism of N(5),N(10)-methenyl-tetrahydromethanopterin cyclohydrolase,
663 Biochemistry, 51 (2012) 8435-8443.
664 [51] V. Carbone, L.R. Schofield, A.K. Beattie, A.J. Sutherland-Smith, R.S. Ronimus, The
665 crystal structure of methenyltetrahydromethanopterin cyclohydrolase from
666 Methanobrevibacter ruminantium, Proteins, 81 (2013) 2064-2070.

667 [52] U. Ermler, C.H. Hagemeier, A. Roth, U. Demmer, W. Grabarse, E. Warkentin, J.A.
668 Vorholt, Structure of Methylene-Tetrahydromethanopterin Dehydrogenase from
669 Methylobacterium extorquens AM1, Structure, 10 (2002) 1127-1137.
670 [53] C.H. Hagemeier, L. Chistoserdova, M.E. Lidstrom, R.K. Thauer, J.A. Vorholt,
671 Characterization of a second methylene tetrahydromethanopterin dehydrogenase from
672 Methylobacterium extorquens AM1, Eur J Biochem, 267 (2000) 3762-3769.
673 [54] L. Chistoserdova, Modularity of methylotrophy, revisited, Environmental Microbiology,
674 13 (2011) 2603-2622.
675 [55] J.T. Keltjens, A. Pol, J. Reimann, H.J. Op den Camp, PQQ-dependent methanol
676 dehydrogenases: rare-earth elements make a difference, Appl Microbiol Biotechnol, 98
677 (2014) 6163-6183.
678 [56] B.K. Pomper, O. Saurel, A. Milon, J.A. Vorholt, Generation of formate by the
679 formyltransferase/hydrolase complex (Fhc) fromMethylobacterium extorquensAM1, FEBS
680 Letters, 523 (2002) 133-137.
681 [57] B.K. Pomper, J.A. Vorholt, Characterization of the formyltransferase
682 fromMethylobacterium extorquensAM1, European Journal of Biochemistry, 268 (2001)
683 4769-4775.
684 [58] O. Rasigraf, D.M. Kool, M.S. Jetten, J.S. Sinninghe Damste, K.F. Ettwig, Autotrophic
685 carbon dioxide fixation via the Calvin-Benson-Bassham cycle by the denitrifying
686 methanotroph "Candidatus Methylomirabilis oxyfera", Appl Environ Microbiol, 80 (2014)
687 2451-2460.
688 [59] F.R. Tabita, T.E. Hanson, H. Li, S. Satagopan, J. Singh, S. Chan, Function, Structure,
689 and Evolution of the RubisCO-Like Proteins and Their RubisCO Homologs, Microbiology
690 and Molecular Biology Reviews, 71 (2007) 576.

691 [60] F.R. Tabita, S. Satagopan, T.E. Hanson, N.E. Kreel, S.S. Scott, Distinct form I, II, III,
692 and IV Rubisco proteins from the three kingdoms of life provide clues about Rubisco
693 evolution and structure/function relationships, J Exp Bot, 59 (2008) 1515-1524.
694 [61] P. Mitchell, Protonmotive redox mechanism of the cytochrome b-c1 complex in the
695 respiratory chain: protonmotive ubiquinone cycle, FEBS Lett, 56 (1975) 1-6.
696 [62] B. Schoepp-Cothenet, R. van Lis, A. Atteia, F. Baymann, L. Capowiez, A.L. Ducluzeau,
697 S. Duval, F. ten Brink, M.J. Russell, W. Nitschke, On the universal core of bioenergetics,
698 Biochim Biophys Acta, 1827 (2013) 79-93.
699 [63] F. ten Brink, B. Schoepp-Cothenet, R. van Lis, W. Nitschke, F. Baymann, Multiple
700 Rieske/cytb complexes in a single organism, Biochimica et Biophysica Acta (BBA) -
701 Bioenergetics, 1827 (2013) 1392-1406.
702 [64] H. Schagger, K. Pfeiffer, Supercomplexes in the respiratory chains of yeast and
703 mammalian mitochondria, The EMBO journal, 19 (2000) 1777-1783.
704 [65] A. Magalon, R. Arias-Cartin, A. Walburger, Supramolecular organization in prokaryotic
705 respiratory systems, Adv Microb Physiol, 61 (2012) 217-266.
706 [66] A.M. Melo, M. Teixeira, Supramolecular organization of bacterial aerobic respiratory
707 chains: From cells and back, Biochim Biophys Acta, 1857 (2016) 190-197.
708 [67] B. Wiseman, R.G. Nitharwal, O. Fedotovskaya, J. Schäfer, H. Guo, Q. Kuang, S.
709 Benlekbir, D. Sjöstrand, P. Ädelroth, J.L. Rubinstein, P. Brzezinski, M. Högbom, Structure of
710 a functional obligate complex III2IV2 respiratory supercomplex from Mycobacterium
711 smegmatis, Nature Structural & Molecular Biology, 25 (2018) 1128-1136.
712 [68] D. Pogoryelov, J. Yu, T. Meier, J. Vonck, P. Dimroth, D.J. Muller, The c15 ring of the
713 Spirulina platensis F-ATP synthase: F_1/F_o symmetry mismatch is not obligatory, EMBO Rep,
714 6 (2005) 1040-1044.

[69] L. Preiss, J.D. Langer, O. Yildiz, L. Eckhardt-Strelau, J.E. Guillemont, A. Koul, T. Meier, Structure of the mycobacterial ATP synthase F_o rotor ring in complex with the anti-TB drug bedaquiline, Science Advances, 1 (2015) e1500106.

Figure Legends

Figure 1: Enzymes involved in the nitrogen metabolism of *M. lanthanidiphila* detected with complexome profiling in DDM (top) or Digitonin (bottom) solubilized membrane samples. Migration profiles using normalized iBAQ values are shown color coded from 0 (black) to 1 (red). The identified proteins with their corresponding identifiers are: NirS (mela_0586), No-d1 (mela_2433), No-d2 (mela_2434), NorZ (mela_0936), sNorII (mela_2377), NapA (mela_0583), NarH2 (mela_2383), NarG2 (mela_2381), NarH1 (mela_0629) and NarG1 (mela_0628).

Figure 2: Protein complexes involved in methane oxidation and carbon fixation from *M. lanthanidiphila*. Migration profiles of identified subunits in DDM (top) and digitonin (bottom) solubilized membranes are reported using normalized iBAQ values, ranging from 0 (black) to 1 (red). The identified proteins with their corresponding identifiers are: PmoC (mela_3065), PmoA (mela_2442), PmoB (mela_2441), XoxF (mela_0916), Fae (mela_2741), MtdB (mela_2742), Mch (mela_2748), FhcD (mela_2746), FhcC (mela_2747), FhcA (mela_2745), FhcB (mela_2744), FwdD (mela_2743), FdhA (mela_1504), FdhB (mela_1503), CbbL (mela_1610) and CbbS (mela_1609).

Figure 3: Migration profiles of the NADH dehydrogenase subunits in DDM (top) or digitonin (bottom) solubilized membranes of *M. lanthanidiphila.* Hierarchical clustering of all identified subunits was performed using normalized iBAQ values, ranging from 0 (black) to 1 (red). The detected subunits of NDH-1(1) with their corresponding identifiers are: NdhA (mela_0372), NdhC (mela_0373), NdhD (mela_0374), NdhH (mela_0375), NdhL (mela_0378), NdhM (mela_0379), NdhN (mela_0380), NdhF (mela_0388), NdhG (mela_2531), NdhI (mela_2529), NdhB (mela_2530). Of NDH-1(2) only the NdhD (mela_0386) and NdhJ (mela_0390) subunits were detected.

Figure 4: Migration profiles of the other respiratory complexes in DDM (top) or digitonin (bottom) solubilized membranes of *M. lanthanidiphila*. Hierarchical clustering of all identified subunits was performed using normalized iBAQ values, ranging from 0 (black) to 1 (red). The detected proteins with their corresponding identifiers are: Qcr1 (mela_1459), CytB (mela_1458), CytC (mela_1457), Cox2 (mela_0200), Cox3 (mela_0198), AtpA (mela_0104), AtpC (mela_0100), AtpD (mela_0101), AtpE (mela_0383), AtpF (mela_0106), AtpG (mela_0102), and AtpH (mela_0105).

Figure 5: Model of the central energy metabolism in *M. lanthanidiphila* that couples oxygen-dependent methane oxidation to nitrite reduction. Nitrite is reduced to nitric oxide (NO) by cytochrome cd_1 nitrite reductase (cd_1-NIR). NO is then potentially dismutated to O_2 and N_2 by a putative NO dismutase (NO-D). This O_2 is consumed by cytochrome *c* oxidase (COX) and used for methane oxidation to methanol by particulate methane monooxygenase (pMMO). Methanol is then oxidized to formaldehyde by methanol dehydrogenase (MDH). Formaldehyde is oxidized to formate or possibly CO_2 by formyltransferase/hydrolase complex (FHC) after being coupled to tetrahydromethanopterin (H_4MPT) via the consecutive action of formaldehyde activating enzyme (FAE), NAD(P)-dependent methylene-tetrahydromethanopterin dehydrogenase (MTD) and methenyl-tetrahydromethanopterin cyclohydrolase (MCH). Formate is oxidized by formate dehydrogenase (FDH). NADH produced by formaldehyde/ formate oxidation is used by a type 1 NADH dehydrogenase (NDH) to produce reduced quinone. These quinones are oxidized by the cytochrome bc_1 complex producing reduced soluble cytochromes, which can donate electrons to COX or cd_1-NIR. The proton-motive force generated by the various respiratory complexes is harvested by ATP synthase to produce ATP. In addition, NO can be reduced to nitrous oxide (N_2O) by nitric oxide reductase (NOR) to prevent nitrosative stress. Theoretically, nitrite can be oxidized to nitrate by nitrite-nitrate oxidoreductase (NXR) or nitrate can be reduced to nitrite by the periplasmic nitrate reductase (NAP) or membrane associated nitrate reductase (NAR), and the responsible protein complexes performing these reactions were detected. However, these last two reactions have not yet been observed in *Methylomirabilis* cells grown under routine growth conditions.

DDM

NirS
No-d1
No-d2
NorZ
sNorI
sNorII
NapA
NapB
NarG1
NarH1
NarI1
NarG2
NarH2
NarI2

cd_1-NIR
NOD 1
NOD 2
qNOR
sNOR
NAP
NAR 1
NAR 2

Membrane
1000 500 100 50
Soluble
1000 500 100 50
Apparent molecular mass(kDa)

Digitonin

NirS
No-d1
No-d2
NorZ
sNorI
sNorII
NapA
NapB
NarG1
NarH1
NarI1
NarG2
NarH2
NarI2

cd_1-NIR
NOD 1
NOD 2
qNOR
sNOR
NAP
NAR 1
NAR 2

Membrane
1000 500 100 50
Soluble
1000 500 100 50
Apparent molecular mass(kDa)

relative abundance

DDM

PmoC
PmoA
PmoB
pMMO
XoxF
La-MDH
Fae
FAE
MtdB
MTD
Mch
MCH
FhcD
FhcC
FhcA
FhcB
FwdD
FHC
FdhA
FdhB
FDH
CbbL
CbbS
RuBisCo

Membrane
1000 500 100 50
Soluble
1000 500 100 50
Molecular mass(kDa)

Digitonin

PmoC
PmoA
PmoB
pMMO
XoxF
La-MDH
Fae
FAE
MtdB
MTD
Mch
MCH
FhcD
FhcC
FhcA
FhcB
FwdD
FHC
FdhA
FdhB
FDH
CbbL
CbbS
RuBisCo

Membrane
1000 500 100 50
Soluble
1000 500 100 50
Molecular mass(kDa)

relative abundance

DDM

NdhA
NdhC
NdhD
NdhH
NdhJ
NdhK
NdhL
NdhM
NdhN
NdhE
NdhF
NdhG
NdhI
NdhB

NDH-1 (1)

NdhD
NdhJ

Membrane
1000 500 100 50

Soluble
1000 500 100 50

Apparent molecular mass(kDa)

Digitonin

NdhA
NdhC
NdhD
NdhH
NdhJ
NdhK
NdhL
NdhM
NdhN
NdhE
NdhF
NdhG
NdhI
NdhB

NDH-1 (1)

NdhD
NdhJ

Membrane
1000 500 100 50

Soluble
1000 500 100 50

Apparent molecular mass(kDa)

relative abundance

DDM

Qcr1
CytB
SuIV
CytC

bc_1 complex

Cox1
Cox2
Cox3

COX

AtpA
AtpB
AtpC
AtpD
AtpE
AtpF
AtpG
AtpH

F-ATPase

Membrane
1000 500 100 50

Soluble
1000 500 100 50

Apparent molecular mass(kDa)

Digitonin

Qcr1
CytB
SuIV
CytC

bc_1 complex

Cox1
Cox2
Cox3

COX

AtpA
AtpB
AtpC
AtpD
AtpE
AtpF
AtpG
AtpH

F-ATPase

Membrane
1000 500 100 50

Soluble
1000 500 100 50

Apparent molecular mass(kDa)

relative abundance

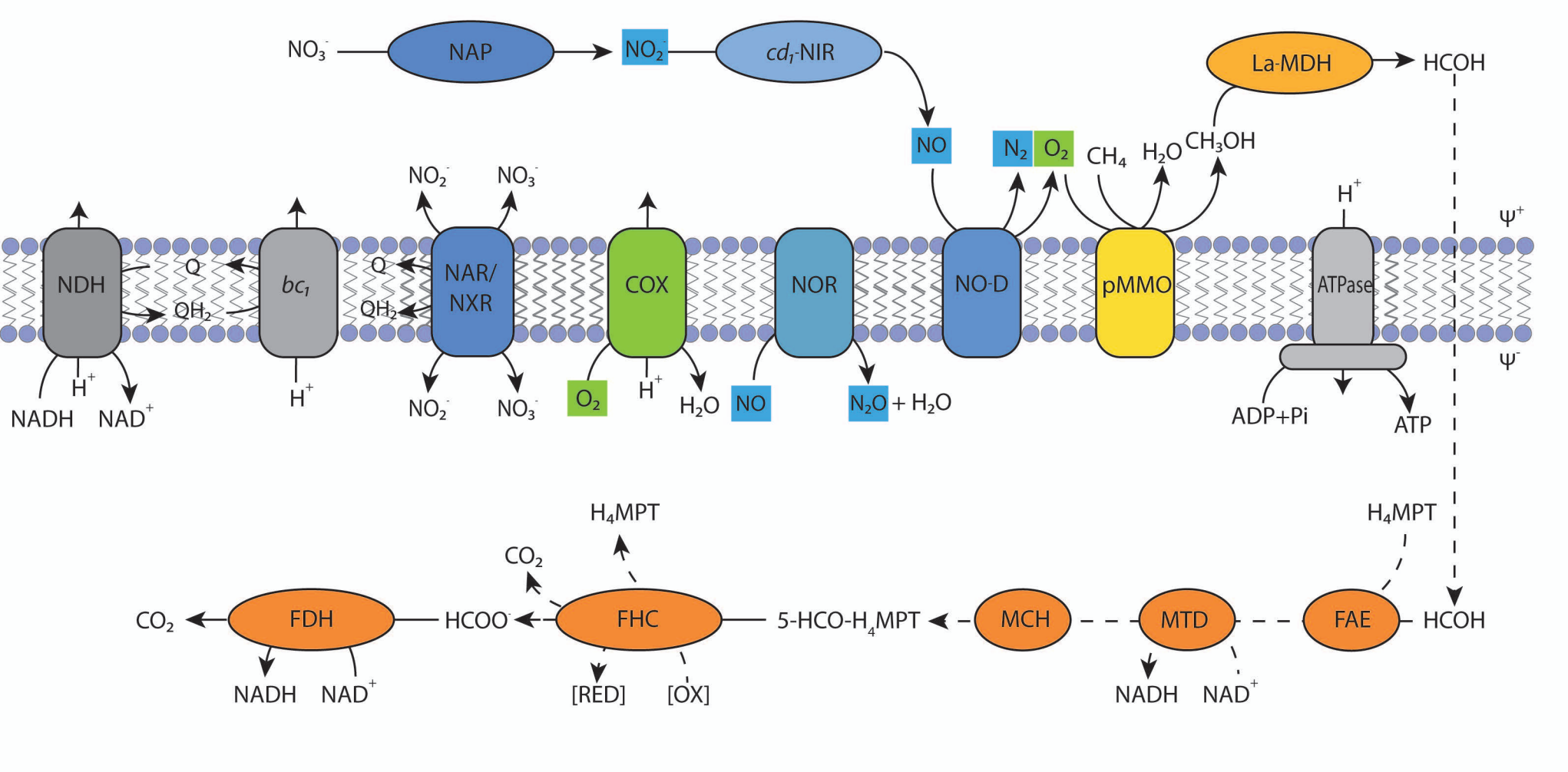
NO3-
NAP
NO2-
cd1-NIR
NO
La-MDH
HCOH
N2
O2
CH4
H2O
CH3OH
NO2-
NO3-
NDH
Q
QH2
bc1
NAR/
NXR
COX
NOR
NO-D
pMMO
H+
ATPase
Ψ+
Ψ-
NADH
NAD+
H+
NO2-
NO3-
O2
H+
H2O
NO
N2O + H2O
ADP+Pi
ATP
H4MPT
CO2
H4MPT
CO2
FDH
HCOO-
FHC
5-HCO-H4MPT
MCH
MTD
FAE
HCOH
NADH
NAD+
[RED]
[OX]
NADH
NAD+